



Quantitative monitoring of circulating tumor DNA in patients with advanced pancreatic cancer undergoing chemotherapy

Makoto Sugimori¹  | Kazuya Sugimori² | Hiromi Tsuchiya² | Yoshimasa Suzuki² | Sho Tsuyuki¹ | Yoshihiro Kaneta¹ | Akane Hirotsu² | Katsuyuki Sanga¹ | Yuichiro Tozuka² | Satoshi Komiyama² | Takeshi Sato²  | Shun Tezuka² | Yoshihiro Goda² | Kuniyasu Irie¹ | Haruo Miwa² | Yuuki Miura² | Tomohiro Ishii² | Takashi Kaneko² | Masatsugu Nagahama³ | Wataru Shibata^{1,4} | Akito Nozaki² | Shin Maeda¹

¹Department of Gastroenterology, Yokohama City University Graduate School of Medicine, Yokohama, Japan

²Gastroenterological Center, Yokohama City University Medical Center, Yokohama, Japan

³Department of Gastroenterology, Showa University Fujigaoka Hospital, Yokohama, Japan

⁴Division of Translational Research, Advanced Medical Research Center, Yokohama City University, Yokohama, Japan

Correspondence

Shin Maeda, Department of Gastroenterology, Yokohama City University Graduate School of Medicine, Yokohama, Japan.
Email: smaeda@yokohama-cu.ac.jp

Funding information

Grant-in-Aid for Scientific Research (KAKENHI), (Grant/Award No: 17K09465) Japan Society for the Promotion of Science

Abstract

According to cancer genome sequences, more than 90% of cases of pancreatic ductal adenocarcinoma (PDAC) harbor active *KRAS* mutations. Digital PCR (dPCR) enables accurate detection and quantification of rare mutations. We assessed the dynamics of circulating tumor DNA (ct-DNA) in patients with advanced PDAC undergoing chemotherapy using dPCR. *KRAS* G12/13 mutation was assayed by dPCR in 47 paired tissue- and ct-DNA samples. The 21 patients were subjected to quantitative ct-DNA monitoring at 4 to 8-week intervals during chemotherapy. *KRAS* mutation was detected in 45 of those 47 patients using tissue DNA. In the *KRAS* mutation-negative cases, next-generation sequencing revealed *KRAS* Q61K and *NRAS* Q61R mutations. *KRAS* mutation was detected in 23/45 cases using ct-DNA (liver or lung metastasis, 18/19; mutation allele frequency [MAF], 0.1%–31.7%; peritoneal metastasis, 3/9 [0.1%], locally advanced, 2/17 [0.1%–0.2%]). In the ct-DNA monitoring, the MAF value changed in concordance with the disease state. In the 6 locally advanced cases, *KRAS* mutation appeared concurrently with liver metastasis. Among the 6 cases with liver metastasis, *KRAS* mutation disappeared during the duration of stable disease or a partial response, and reappeared at the time of progressive disease. The median progression-free survival was longer in cases in which *KRAS* mutation disappeared after an initial course of chemotherapy than in those in which it was continuously detected (248.5 vs 50 days, $P < .001$). Therefore, ct-DNA monitoring enables continuous assessment of disease state and could have prognostic utility during chemotherapy.

KEYWORDS

biomarker, circulating tumor DNA, digital PCR, *KRAS*, pancreatic ductal adenocarcinoma

This is an open access article under the terms of the Creative Commons Attribution-NonCommercial License, which permits use, distribution and reproduction in any medium, provided the original work is properly cited and is not used for commercial purposes.

© 2019 The Authors. *Cancer Science* published by John Wiley & Sons Australia, Ltd on behalf of Japanese Cancer Association.

1 | INTRODUCTION

Pancreatic ductal adenocarcinoma (PDAC) has a high mortality rate and its incidence is increasing.¹ Both early clinical diagnosis and confirmatory pathological diagnosis of PDAC are problematic. Several diagnostic techniques for PDAC have been developed. Among them, endoscopic ultrasound-guided fine-needle aspiration (EUS-FNA) has dramatically improved the sensitivity and accuracy of PDAC diagnosis.² However, pathological diagnosis is hampered by the small specimen and low purity of tumor cells. Indeed, differential diagnosis of pancreatic solid masses by EUS-FNA is challenging in approximately 15% of cases.^{3,4}

Activating *KRAS* mutations were found in more than 90% cases of PDAC and accumulated on codons 12 and 13 (Figure S1).⁵⁻⁸ These activating *KRAS* mutations are reported to impair intrinsic GTPase activity and block the interaction between *KRAS* and GTPase-activating proteins, leading to constitutive activation of oncogenic signaling pathways and induction of proliferation, metabolism, and metastasis.⁹ Furthermore, almost all PDACs develop in a pancreatic intraepithelial neoplasia (PanIN)-dependent manner and activating *KRAS* mutations are found in low-grade PanIN 1A lesions.^{10,11} To improve the diagnostic accuracy of PDAC, several prior studies tested for *KRAS* mutations using EUS-FNA samples such as Sanger sequencing (sensitivity, ~10%), real time-quantitative PCR (~1%), amplification-refractory mutation system (~1%), mutant enriched PCR (~0.1%),^{3,12-14} and next-generation sequencing (NGS; ~1-5%).¹⁵⁻¹⁸

Detection of *KRAS* mutations using EUS-FNA samples is useful for initial diagnosis. However, it is not always repeatable and is a specific technique. Tumor-derived DNA circulates in the blood.¹⁹ A *KRAS* mutation at codon 12 and 13, which is harbored by the majority of PDACs, could be a surrogate marker for circulating tumor DNA (ct-DNA). Furthermore, the amount of ct-DNA likely reflects the total tumor volume (primary and metastatic lesions), so quantitative monitoring of ct-DNA could facilitate continuous evaluation of the treatment response and early detection of resistance to chemotherapy, and so improve the clinical outcomes.²⁰

Digital PCR (dPCR), which is efficient and accurate, is based on the compartmentalization of DNA samples into 20 000-30 000 microdroplets, microchambers, or microwells. This enables amplification, detection, and quantification of rare mutations. Digital PCR allows genetic testing using a small amount of ct-DNA for the diagnosis and treatment of cancer.²¹

We assessed the dynamics of ct-DNA in patients with advanced PDAC undergoing chemotherapy using dPCR and evaluated the utility of ct-DNA monitoring.

2 | MATERIALS AND METHODS

2.1 | Subjects and samples

A total of 54 EUS-FNA tissue samples were collected from patients with a pancreatic tumor who underwent EUS-FNA due to suspicion

of PDAC based on imaging findings (computed tomography [CT] or MRI). The final pathological diagnoses were 47 cases of PDAC and 7 of neuroendocrine tumor (NET). Serum samples were collected from 47 patients with PDAC (female, N = 19; male, N = 28; age, 66 [27-78] years). The baseline characteristics of the 47 patients with PDAC are shown in Table 1 and Table S1. Among them, from 21 subjects (female, N = 7; male, N = 14; age, 64 [27-78] years), serum samples were collected every 4-8 weeks following chemotherapy. Blood samples were obtained by venous puncture and were assayed for the levels of tumor markers (carcinoembryonic antigen [CEA] and carbohydrate antigen 19-9 [CA19-9]). The tumor response to chemotherapy was evaluated by imaging according to the RECIST 1.1 criteria.

The subjects were prospectively recruited at Yokohama City University Hospital and Yokohama City University Medical Center. This prospective multicenter cohort study was approved by the Regional Committee for Medical and Health Research Ethics of Yokohama City University, and all patients provided informed consent prior to EUS-FNA and chemotherapy.

2.2 | Preparation of DNA from tissue and serum samples

The EUS-FNA tissues were obtained using a 22-gauge needle. Tissue samples were collected during biopsy for the purpose of histopathological diagnosis and were stored at -80°C in 1 mL RNAlater (#AM7021; Thermo Fisher Scientific). DNA was extracted using a QIAamp DNA Mini Kit (#51304; Qiagen) according to the manufacturer's instructions. Blood samples were collected in tubes containing a clot activator and polyolefin gel (Venoject II, VP-AS109K50; Terumo), which is usually used for clinical blood chemistry testing. The blood samples were left to stand for 30 minutes and centrifuged for 10 minutes at 1760 g. The supernatant was collected and stored at -80°C. Before ct-DNA isolation, the samples were dissolved on ice and centrifuged for 10 minutes at 22 140 g. The supernatant was collected carefully, and 2-3 mL was used for extraction of ct-DNA using a QIAamp Circulating Nucleic Acid Kit (#55114, Qiagen) according to the manufacturer's instructions. The DNA concentration was assayed using the Qubit dsDNA HS Kit and a Qubit 3.0 fluorometer (#Q33231; Thermo Fisher Scientific).

2.3 | Detection of mutations by dPCR

To detect *KRAS* mutation by dPCR in tissue- or ct-DNA samples, we used the LBx Probe for *KRAS* G12/13 (A183; Riken Genesis), which can detect 16 *KRAS* mutation patterns (p.G12A/C/D/F/G/L/R/S/V, p.G13A/C/D/G/R/S/V). In a case with WT *KRAS* and *NRAS* Q61R mutation revealed by NGS analysis, we used the LBx Probe for *NRAS* Q61 (A096; Riken Genesis), which can detect seven *NRAS* mutation patterns (p.Q61R/K/L/H/P/E, p.E62K). Digital PCR was carried out according to the manufacturer's instructions using 20 ng tissue DNA or more than 10 ng of ct-DNA and the QX200

TABLE 1 Baseline characteristics of 47 patients with pancreatic ductal adenocarcinoma

	Total	Locally advanced	Peritoneal metastasis	Liver or lung metastasis
N	47	17	9	21
Gender; female, male	19, 28	8, 9	4, 5	7, 14
Age, years; average	66	69	70	63
(range)	(27-78)	(57-77)	(56-77)	(27-78)
Stage	4, 3, 10, 30	4, 3, 10	9	21
(UICC 7th)	(IIA, IIB, III, IV)	(IIA, IIB, III)	(IV)	(IV)
Location; H, B, T	28, 9, 10	15, 2, 0	5, 1, 3	8, 6, 7
CEA, ng/mL; average \pm SD	33.4 \pm 98.8	6.5 \pm 9.3	15.8 \pm 26.7	62.7 \pm 141.0
CEA > 5 ng/mL	26	7	4	15
CA19-9, U/mL; average \pm SD	12 769.2 \pm 57 044.1	1232.3 \pm 3336.8	5255.7 \pm 7834.4	25 328.8 \pm 83 413.6
CA19-9 > 37 U/mL	41	14	9	18

Abbreviations: B, body; CA19-9, carbohydrate antigen 19-9; CEA, carcinoembryonic antigen; H, head; T, tail.

instrument (Bio-Rad); the data were analyzed using Quanta Soft software (Bio-Rad). We calculated the mutation allele frequency (MAF) value, the ratio of the number of FAM-negative and HEX-positive droplets (indicating mutated KRAS G12/13) to the total number of FAM- and/or HEX-positive droplets (no mutated or mutated KRAS G12/13) (Figure 1A).

To validate the dPCR data, DNA extracted from human 293T and MIA PaCa-2 cells was used. The Cancer Cell Line Encyclopedia²² (Wellcome Trust, <https://portals.broadinstitute.org/ccle>) database showed that 293T cells have WT KRAS, whereas MIA PaCa-2 cells are homozygous for KRAS G12C.²³ DNA was extracted using a QIAamp DNA Mini Kit (#51304; Qiagen) according to the manufacturer's instructions. A dPCR KRAS copy number variation (CNV) assay was carried out using Prime PCR probes for KRAS and RPP30 (#10031240, #10031244; Bio-Rad); the latter was used as a reference and is present at 2 copies per diploid genome. The ratio of KRAS to RPP30, which indicates CNV of KRAS, was almost equal to 1 in both cell types (data not shown). Next, we adjusted the DNA concentration of MIA PaCa-2 cells by adding that of 293T (Table S2) and detected KRAS mutations by dPCR using the LBx Probe. This dPCR mutation detection assay can detect as little as 0.1% mutant allele in a WT allele background, and the MAF value was correlated with that estimated by dilution. Therefore, we defined the lower limit of detection as 0.1%, and samples with MAF values higher than 0.1% were considered positive for KRAS mutation (Table S2).

2.4 | Next-generation sequencing analysis

In the 2 cases of PDAC in which no KRAS G12/13 mutation was detected by dPCR, NGS was carried out using the Ion Ampli-seq Cancer Hotspot Panel version 2 (CHPv2) (#20019161; Illumina) and the iSeq100 system (Illumina). The data were analyzed using BaseSpace

Sequence Hub software (Illumina) and compared with normal DNA from PBMCs.

2.5 | Statistical analysis

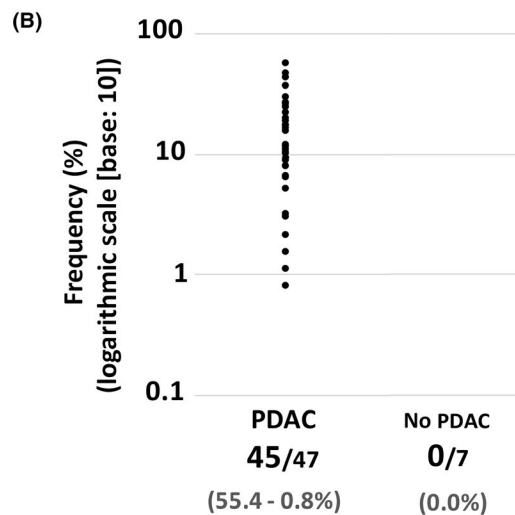
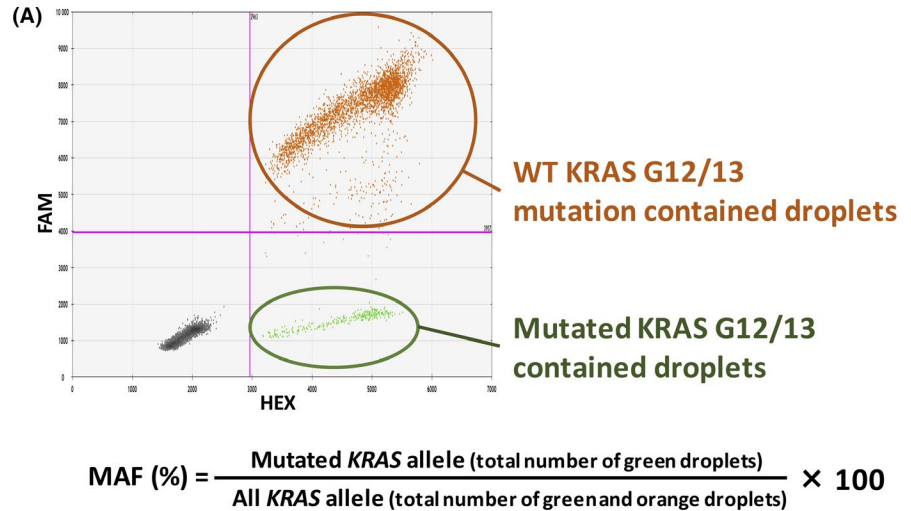
Progression-free survival (PFS) was defined as the time from the start of chemotherapy to that of the first event (evaluated as progressive disease [PD] according to RECIST 1.1 criteria). Patients who did not progress during the follow-up period were censored. Progression-free survival was evaluated using the Kaplan-Meier method and was compared by log-rank test and presented as hazard ratios and 95% confidence intervals. The Kruskal-Wallis test was used to compare KRAS-MAF across the 3 disease stage groups (locally advanced, peritoneal metastasis, and liver or lung metastasis). Changes in KRAS-MAF and tumor marker (CEA and CA19-9) levels over time were compared by Wilcoxon matched-pairs signed-rank test. Correlation tests were carried out between the change of KRAS-MAF and tumor marker levels by the non-parametric Spearman's rank correlation coefficient test. A 2-sided *P* value of less than 0.05 was considered indicative of statistical significance. Statistical analysis was undertaken using Prism 7 (GraphPad Software).

3 | RESULTS

3.1 | Detection of KRAS mutations by dPCR and NGS analysis in tissue DNA samples

We evaluated KRAS mutations in EUS-FNA tissue DNA samples by dPCR. KRAS mutation was detected in 45/47 cases of PDAC and 0/7 cases of NET, pathologically diagnosed (Figure 1B). In the 2 cases of no KRAS G12/13 mutation detected PDAC, NGS analysis confirmed

FIGURE 1 A, A typical case of *KRAS* G12/13 mutation detected by digital PCR (dPCR). FAM- and HEX-positive droplets (orange) indicate WT *KRAS* codon 12/13 DNA fraction; FAM-negative, HEX-positive (green) droplets indicate mutated *KRAS* codon G12/13 DNA fraction. B, Detection of mutated *KRAS* G12/13 by dPCR in 54 tissue DNA samples (pancreatic ductal adenocarcinoma [PDAC], 47; neuroendocrine tumor [NET], 7). *KRAS* mutation was detected in 45/47 PDAC samples (mutation allele frequency [MAF], 55.4%-0.8%), whereas no *KRAS* mutation was detected in non-PDAC samples



no *KRAS* G12/13 mutation and revealed 1 case harbored *KRAS* Q61K (MAF, 38%) and *TP53* R213Ter (84%) (Table 2; Table S1, patient [Pat.] #46), and the other harbored *NRAS* Q61R (52%) (Table 2; Table S1, Pat. #47). The disease history and findings of Pat. #47 are described below (representative case 3).

3.2 | Detection of *KRAS* mutation by dPCR in ct-DNA samples

The *KRAS* G12/13 mutation detection by dPCR was carried out on ct-DNA samples extracted from the serum of 45 PDAC patients with *KRAS* G12/13 mutation, detected in tissue DNA analysis. A preliminary validation study revealed that the lower limit of detection was 0.1% (Table S2), and so samples with a MAF value greater than 0.1% were considered positive for *KRAS* mutation. *KRAS* mutation was detected in 2/17 cases of local progression (MAF, 0.1%-0.2%), 3/9 cases of peritoneal metastasis (MAF, 0.1%), and 18/19 cases of liver or lung metastasis (MAF, 0.1%-31.7%) (Figure 2). The patients with liver or lung metastasis had higher MAF than those with locally advanced or peritoneal metastatic disease ($P < .001$).

TABLE 2 Somatic mutations identified by next-generation sequencing analysis in 2 cases of pancreatic ductal adenocarcinoma without *KRAS* G12/13 mutation detected in digital PCR analysis

Gene	Mutation	MAF	Clin Var
#46			
<i>KRAS</i>	p.Q61K	38%	Pathogenic
<i>TP53</i>	p.R213Ter	84%	Pathogenic
#47			
<i>NRAS</i>	p.Q61R	52%	Pathogenic

Note: Clin Var, Wellcome trust database provided by NCBI (<https://www.ncbi.nlm.nih.gov/clinvar/>); MAF, mutation allele frequency.

3.3 | Association of baseline tumor marker levels or *KRAS* mutation detection in ct-DNA with outcomes

Among the 45 PDAC patients with *KRAS* G12/13 mutation, 31 underwent chemotherapy. The patients with baseline of tumor markers equal to or above the median value (CEA, 5.6 mg/mL; CA19-9, 623.0 U/mL) tended to have a worse PFS than those with baseline below the

median value (CEA, median 244 vs 195 days, $P = .20$; CA19-9, median 281 vs 169 days, $P = .10$) (Figure 3A,B). Also, the patients with *KRAS* mutation detected in ct-DNA at the time of diagnosis ($N = 19$) tended to have a worse PFS than those with no *KRAS* mutation detected ($N = 12$) (median 308.5 vs 168 days, $P = .07$) (Figure 3C).

3.4 | Quantitative monitoring of *KRAS* or *NRAS* mutation in ct-DNA

Of the 21 PDAC patients with *KRAS* or *NRAS* mutation in the primary tumor (8 locally advanced and 13 liver or lung metastasis), serum samples were collected every 4-8 weeks for quantitative monitoring of *KRAS* or *NRAS* mutation in ct-DNA from patients undergoing chemotherapy. The baseline characteristics of the patients are shown in Table 3. *KRAS*-MAF values determined by dPCR were followed up and compared with the tumor marker levels and the therapeutic response was evaluated by imaging according to the RECIST 1.1 criteria.

Swimmer plots of chemotherapy with ct-DNA monitoring are shown in Figure 4. Among the 8 locally advanced cases, a *KRAS* mutation in ct-DNA was detected in 2 cases at the time of diagnosis (Pat. #16, 17). In these cases, the *KRAS* mutation disappeared during chemotherapy, but reappeared at the time of PD with liver metastasis. The other 6 locally advanced cases showed no *KRAS* mutation in ct-DNA at the time of diagnosis. Among them, 4 cases were detected *KRAS* mutation in ct-DNA for the first time at the same time that liver metastasis appeared or earlier (Pat. #10, 11, 12, 15). In the two case, no *KRAS* mutation was detected at the time 1st PD, due to the enlargement of primary lesion with no

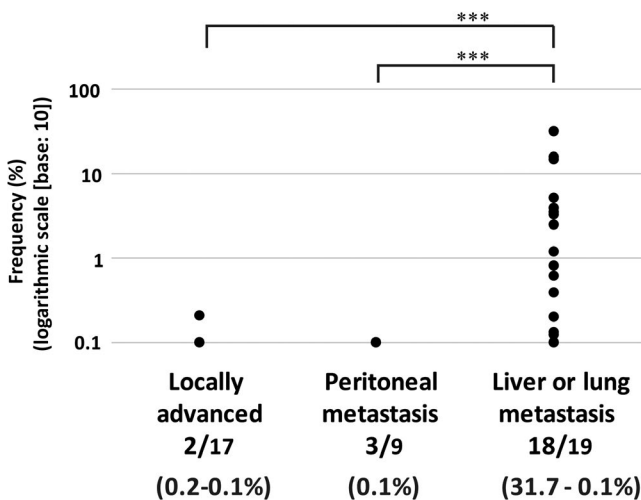
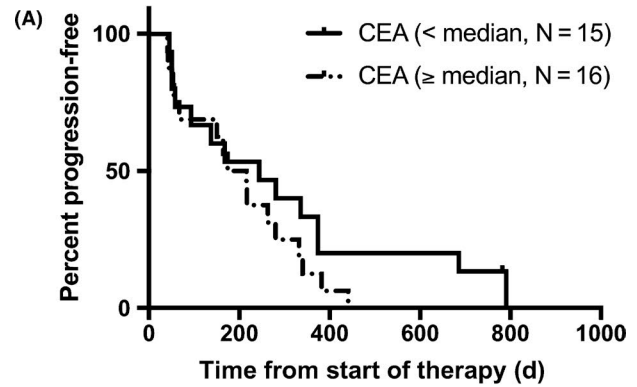
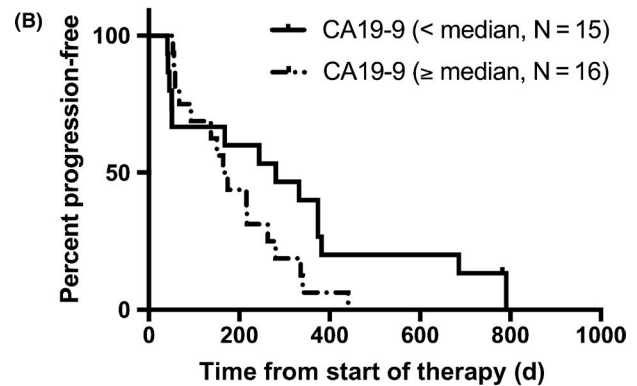


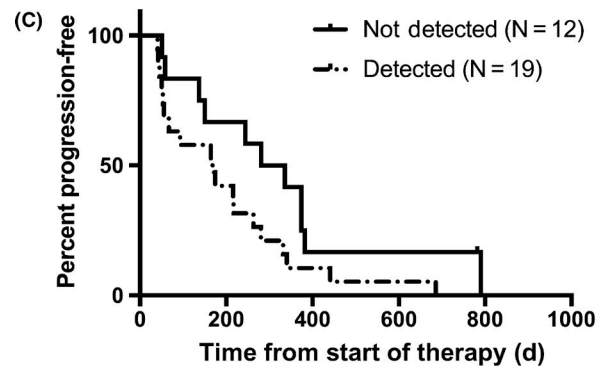
FIGURE 2 Detection of *KRAS* G12/13 mutation by digital PCR in circulating tumor DNA samples at the time of diagnosis. *KRAS* mutation was detected in 2/17 locally advanced cases (mutation allele frequency [MAF], 0.1%-0.2%), 3/9 peritoneal metastasis cases (MAF, 0.1%), and 18/19 liver or lung metastasis cases (MAF, 31.7%-0.1%). Those patients with liver or lung metastasis had higher MAF than patients with locally advanced or peritoneal metastatic disease, by Kruskal-Wallis test ($***P < .001$)



HR, 1.641; 95% CI, 0.7551-3.215; $P = .20$



HR, 1.74; 95% CI, 0.08374-3.617; $P = .10$



HR, 1.973; 95% CI, 0.9631-4.043; $P = .07$

FIGURE 3 A,B, Kaplan-Meier plot of progression-free survival (PFS) during first-line chemotherapy of cases with baseline of tumor markers below and, equal to or above the median value (carcinoembryonic antigen [CEA], median 244 vs 195 days, $P = .20$; carbohydrate antigen 19-9 [CA19-9], median 281 vs 169 days, $P = .10$). C, Kaplan-Meier plot of PFS during first-line chemotherapy of cases with ($N = 19$) and without ($N = 12$) *KRAS* G12/13 mutation in circulating tumor DNA (ct-DNA) at the time of diagnosis (in tissue, *KRAS* G12/13 mutation was detected in all 31 cases). The cases, *KRAS* mutation detected in the ct-DNA, had a nonsignificantly worse PFS than those without *KRAS* mutation (median 308.5 vs 168 days, $P = .07$). CI, confidence interval; HR, hazard ratio

distant metastasis (Pat. #12, 13). In the case of Pat. #14, no ct-DNA sample was obtained at the time of first PD. However, the *KRAS* mutation appeared at the second PD, due to the enlargement of liver metastatic lesions.

Among the 12 cases with lung or liver metastasis, *KRAS* mutation in ct-DNA was detected in 11 cases at the time of diagnosis (the exception being Pat. #34). In the 6 cases with liver metastasis (Pat. #35, 36, 37, 38, 39, 40), *KRAS* mutation disappeared after the initial course of chemotherapy. During the following period, the tumor response evaluated as stable disease (SD) or partial response (PR), no *KRAS* mutation was detected, and *KRAS* mutation reappeared concurrently with or earlier than PD. In the other 5 cases, *KRAS* mutation did not disappear from the time of diagnosis to that of first PD (Pat. #41, 42, 43, 44, 45). The median PFS was significantly longer in cases in which *KRAS* mutation disappeared after the initial course of chemotherapy than in those in which it remained (248.5 vs 50 days, $P < .001$) (Figure 5). In a case with *NRAS* Q61R mutation detected by NGS, the MAF value of *NRAS* Q61 mutation was followed up (Pat. #47). The MAF value changed in concordance with the therapeutic response

evaluated by CT. The clinical course is described below (representative case #3).

3.5 | Correlation of *KRAS*-MAF with tumor markers

To evaluate the utility of the *KRAS*-MAF value as a tumor marker, we compared the changes in the *KRAS*-MAF value with those in the CEA and CA19-9 levels. In the responder group, *KRAS* mutation disappeared ($N = 8$; Pat. #16, 17, 35, 36, 37, 38, 39, 40), the *KRAS*-MAF value and the levels of CEA and CA19-9 significantly decreased after the initial course of chemotherapy (Figure 6A). Similarly, in patients with *KRAS* mutation ct-DNA monitoring ($N = 20$), the *KRAS*-MAF value and the levels of CEA and CA19-9 significantly increased in the time of first PD, compared to those at the time 1 course of chemotherapy before (Figure 6B). Furthermore, in each case with these timings (before vs after initial course of chemotherapy, and 1 course of chemotherapy before vs after first PD), there was significant correlation between the change of *KRAS*-MAF values (Δ *KRAS*-MAF) and those of CEA and CA19-9 levels (%change) (Figure 6C).

TABLE 3 Characteristics of patients with pancreatic ductal adenocarcinoma who underwent circulating tumor DNA (ct-DNA) monitoring

	Total	<i>KRAS</i> G12/13 mutated cases			<i>NRAS</i> -mutated case	
		Not detected in ct-DNA at time of diagnosis	Detected in ct-DNA at the time of diagnosis			
			Total	Disappeared	Remained	
N	21	7	13	8	5	1
Gender; female, male	7, 14	3, 4	3, 10	3, 5	0, 5	1, 0
Age, years; average (range)	64 (27-78)	67 (57-74)	65 (42-78)	64 (42-77)	67 (57-78)	27 (27)
Stage (UICC 7th)	1, 7, 13 (IIB, III, IV)	1, 5, 1 (IIB, III, IV)	2, 11 (III, IV)	2, 6 (III, IV)	5 (IV)	1 (IV)
<i>KRAS</i> G12/13 mutation in tissue DNA	Yes, 20	Yes, 7	Yes, 13	Yes, 8	Yes, 5	Yes, 0
	No, 1 (<i>NRAS</i> Q61R detected)	No, 0	No, 0	No, 0	No, 0	No, 1 (<i>NRAS</i> Q61R detected)
MAF in ct-DNA (%) at the time of diagnosis (<i>KRAS</i> or <i>NRAS</i>), average \pm SD	2.8 \pm 7.1	0.0 \pm 0.0	2.2 \pm 3.9	3.1 \pm 4.7	0.9 \pm 1.2	31.2 \pm 0.0
1st regimen	GN, 18	GN, 5	GN, 12	GN, 8	GN, 4	GN, 1
	mFFX, 1	mFFX, 1	GEM, 1		GEM, 1	
	GEM, 1 S1, 1	S1, 1				
CEA, ng/mL; average \pm SD	42.7 \pm 136.4	6.0 \pm 4.0	65.7 \pm 169.3	21.7 \pm 20.4	55 476.0 \pm 128 563.7	1.8 \pm 0.0
CEA > 5 ng/mL	15	4	11	7	4	0
CA19-9 (U/mL) Ave. \pm SD	22 165.8 \pm 63 597.2	2330.1 \pm 4968.2	34 550.6 \pm 104 272.8	136.0 \pm 256.5	1070.0 \pm 1409.6	12.0 \pm 0.0
CA19-9 > 37 U/mL	17	6	11	7	4	0

Abbreviations: CA19-9, carbohydrate antigen 19-9; CEA, carcinoembryonic antigen; GEM, gemcitabine; GN, gemcitabine plus nab-paclitaxel; MAF, mutation allele frequency; mFFX, modified FOLFIRINOX; S1, tegafur (masked compound of 5-fluorouracil).

The KRAS-MAF values and the levels of CEA and CA19-9 are individually shown in Table S3. In the comparison of biomarkers, however, CEA or CA19-9 non-elevated cases (CEA < 5.0 ng/mL, CA19-9 < 37.0 U/mL) and no ct-DNA sample obtained at the time of first PD case (Pat. #14) needed to be omitted.

3.6 | Representative case 1 (Pat. #10)

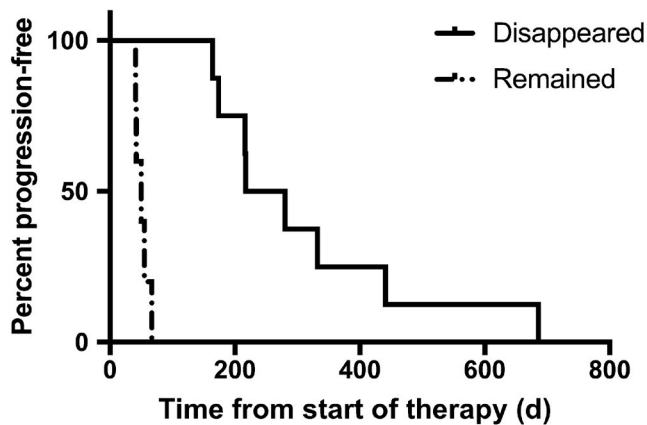
A 57-year-old woman with a history of type 2 diabetes mellitus presented to a local outpatient clinic complaining of back pain and weight loss. Abdominal ultrasonography revealed cancer of the pancreatic head, and she was referred to our hospital. Laboratory data revealed high levels of serum bilirubin (total bilirubin, 10.9 mg/dL; direct bilirubin, 8.0 mg/dL), liver enzymes (alanine transaminase

[ALT], 131.0 U/L; aspartate transaminase [AST], 263 U/L), and tumor markers (CEA, 13.4 ng/mL; CA19-9, 294.0 U/mL). Computed tomography findings revealed a 30 × 19 mm mass in the pancreatic head with malignant biliary obstruction, and that the common hepatic artery (CHA) was encased by the tumor. After placement of a plastic stent for biliary drainage, EUS-FNA resulted in a pathologic diagnosis of pancreatic adenocarcinoma. Therefore, the patient was diagnosed with stage IIB (T3N1M0, UICC 7th) PDAC. Gemcitabine and nab-paclitaxel (GEM plus nab-PTX) treatment was initiated as the first-line regimen (day 45). On day 427, after 21 courses of treatment, the response was evaluated as PD due to appearance of a new hepatic metastatic lesion, and second-line modified FOLFIRINOX (mFFX) therapy²⁴ was initiated on day 440. On day 560, after 4 courses of treatment, the tumor response was evaluated as PD due to enlargement of the hepatic metastatic lesion.

The swimmer plots of chemotherapy treated PDAC patients, ct-DNA monitoring performed.



FIGURE 4 Swimmer plots of chemotherapy-treated pancreatic ductal adenocarcinoma (PDAC) cases classified into the following groups: (1) KRAS G12/13 mutation detected in tissue DNA but not in circulating tumor DNA (ct-DNA) at the time of diagnosis (N = 7); (2) KRAS G12/13 mutation detected in both tissue DNA and ct-DNA at the time of diagnosis (N = 13); and (3) NRAS Q61R mutation detected by next-generation sequencing (N = 1). Chemotherapy regimens are indicated by colored bars. Filled red circles with value, KRAS or NRAS mutation detected with mutation allele frequency (MAF) values; unfilled red circles, not detected. Blue and white flags, times of RECIST progressive disease (PD) due to appearance or enlargement of distant metastasis and to enlargement of the primary lesion, respectively. FFX, FOLFIRINOX; GEM, gemcitabine; nab-PTX, nab-paclitaxel; PFS, progression-free survival; S1, tegafur (a masked compound of 5-fluorouracil)



HR, 56.67; 95% CI, 7.311-439.3; $P < .001$

FIGURE 5 Kaplan-Meier plot of progression-free survival (PFS) in pancreatic ductal adenocarcinoma cases in which *KRAS* G12/13 mutation in circulating tumor DNA (ct-DNA) disappeared ($N = 8$) or remained ($N = 5$) after the initial course of first-line chemotherapy. Cases in which *KRAS* G12/13 mutation in ct-DNA remained had a significantly worse PFS than those in which it disappeared (median 248.5 vs 50 days, $P = .001$). CI, confidence interval; HR, hazard ratio

KRAS G12/13 mutation was detected by dPCR in EUS-FNA samples, therefore, serum samples were collected every 4-8 weeks and *KRAS* mutation was monitored in ct-DNA (Figure 7).

In samples at the time of diagnosis and in 6 obtained subsequently, no *KRAS* mutation was detected. Interestingly, in the day 364 sample, when the tumor response was evaluated as SD, *KRAS* mutation was detected (MAF, 0.2%). Furthermore, in the day 434 sample, when the tumor response was evaluated as PD, the *KRAS*-MAF value was elevated (1.7%). The increase in the *KRAS*-MAF value was concurrent with that in the CEA and CA19-9 levels. The CEA and CA19-9 levels increased during second-line chemotherapy; however, the *KRAS*-MAF value decreased transiently and subsequently increased at the time of PD.

3.7 | Representative case 2 (Pat. #39)

A 59-year-old woman presented to a local outpatient clinic complaining of bowel distention and loss of appetite. Abdominal ultrasonography revealed multiple liver masses, and she was referred to our hospital. Laboratory data revealed high levels of liver enzymes (ALT, 219.0 U/L; AST, 271 U/L) and tumor markers (CEA, 59.9 ng/mL; CA19-9, 394 500.0 U/mL). Computed tomography findings revealed a 61 × 32 mm mass in the pancreatic tail with multiple liver and lung metastases. The celiac artery, superior mesenteric artery, and splenic artery were encased by the tumor. Pancreatic adenocarcinoma was diagnosed based on the pathologic findings of an EUS-FNA sample. Therefore, the patient was diagnosed with stage IV (T4N1M1, UICC 7th) PDAC. Gemcitabine plus nab-PTX was started as the first-line regimen (day 0). On day

176, after 9 courses of treatment, the tumor response was evaluated as PD due to the appearance of a new hepatic metastatic lesion, and mFFX treatment was started as the second line on day 187. On day 218, after 1 course of treatment, the tumor response was evaluated as PD due to enlargement of the hepatic metastatic lesion. On day 219, GEM plus S1 (tegafur, a masked compound of 5-fluorouracil) treatment was started as the third line, and the tumor response was evaluated as PD due to enlargement of the hepatic metastatic lesion on day 260.

KRAS G12/13 mutation was detected by dPCR. Therefore, we quantitatively monitored *KRAS* mutation in ct-DNA every 4 to 8 weeks (Figure 8). *KRAS* mutation was detected at the time of diagnosis (MAF, 14.5%). Interestingly, in the following 2 samples, *KRAS* mutation had disappeared. In the day 134 sample, when the tumor response was evaluated as PR, *KRAS* mutation reappeared (0.4%). Furthermore, in the day 170 sample, when the tumor response was evaluated as PD, the *KRAS*-MAF value was elevated (1.4%). The timing of the increase in *KRAS*-MAF was identical to that of the elevation of the CEA and CA19-9 levels. During subsequent second- or third-line chemotherapy, *KRAS* mutation was detected continuously and the tumor response was evaluated as PD after only 1 course of chemotherapy treatment in each regimen.

3.8 | Representative case 3 (Pat. #47)

A 27-year-old woman with no obvious medical or familial history presented to a local outpatient clinic complaining of epigastric pain. Abdominal ultrasonography revealed multiple liver masses, and she was referred to our hospital. Laboratory data revealed elevated liver enzyme levels (ALT, 108.0 U/L; AST, 174 U/L), but those of tumor markers—CEA (1.8 ng/mL), CA19-9 (12.0 U/mL), Dupan-2 (70.0 U/mL), and Span-1 (11.0 U/mL)—were within the normal limits. The CT findings revealed a 44.5 × 35 mm mass in the pancreatic tail with multiple liver metastases. In addition, the CHA, portal vein, superior mesenteric vein, and splenic vein were encased by the tumor. The EUS-FNA resulted in a diagnosis of pancreatic adenocarcinoma. Immunohistochemical analysis showed that the tumor cells were positive for CK7 and negative for CK20. Therefore, the patient was diagnosed with stage IV (T4N1M1, UICC 7th) PDAC. Gemcitabine plus nab-PTX treatment was started as the first-line regimen and the tumor volume dramatically decreased. The tumor response was evaluated as PR after day 116 until the time of writing (day 475).

No *KRAS* G12/13 mutation was detected by dPCR. The NGS analysis using CHPv2 revealed *NRAS* Q61R. Therefore, we monitored the *NRAS* Q61 mutation in ct-DNA at 4- to 8-week intervals (Figure 9). At the time of diagnosis, *NRAS* mutation was detected (MAF, 31.2%). During chemotherapy, the MAF value decreased dramatically (day 68, 0.3%; day 116, 0.1%). From day 214 to the time of writing (day 475), no *NRAS* mutation was detected in ct-DNA samples.

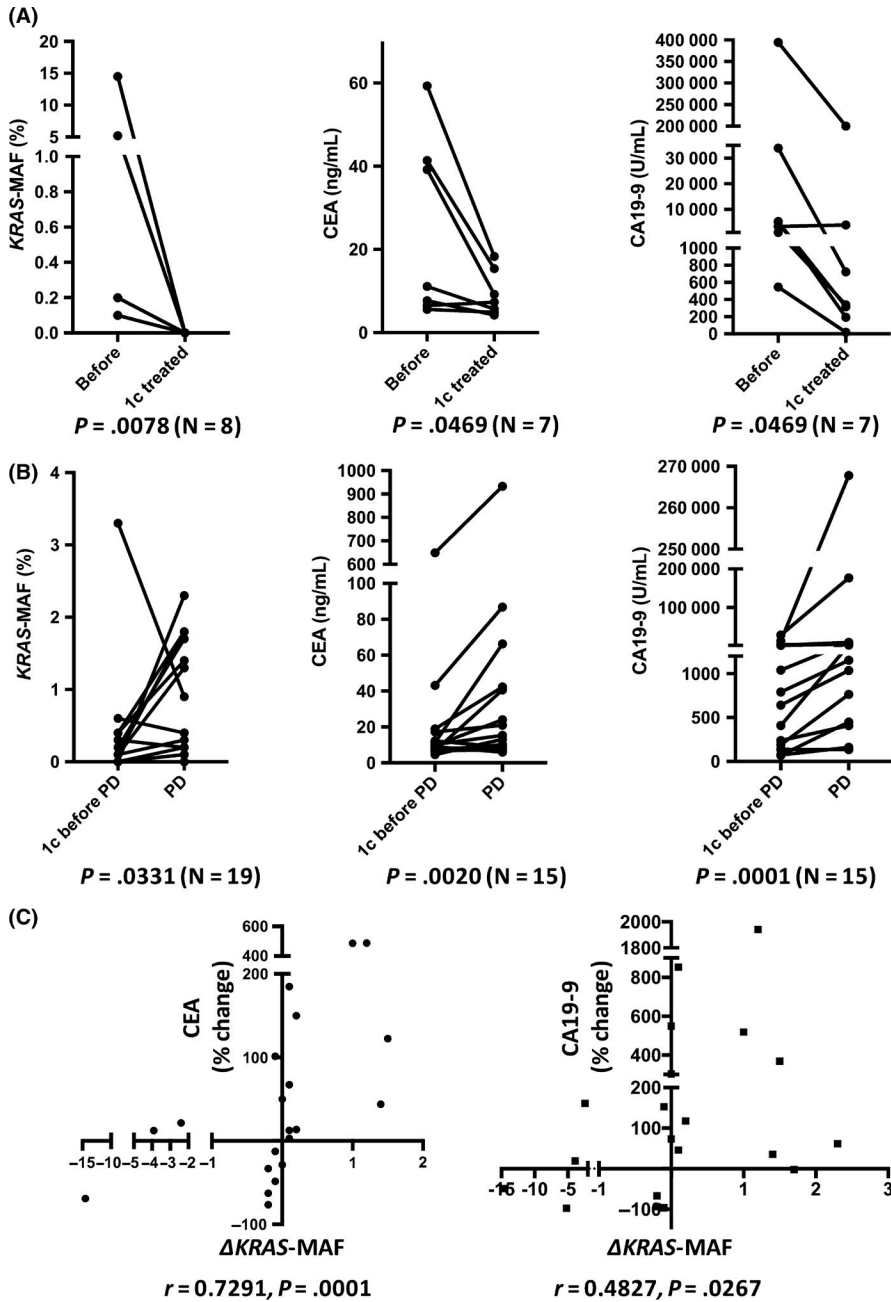


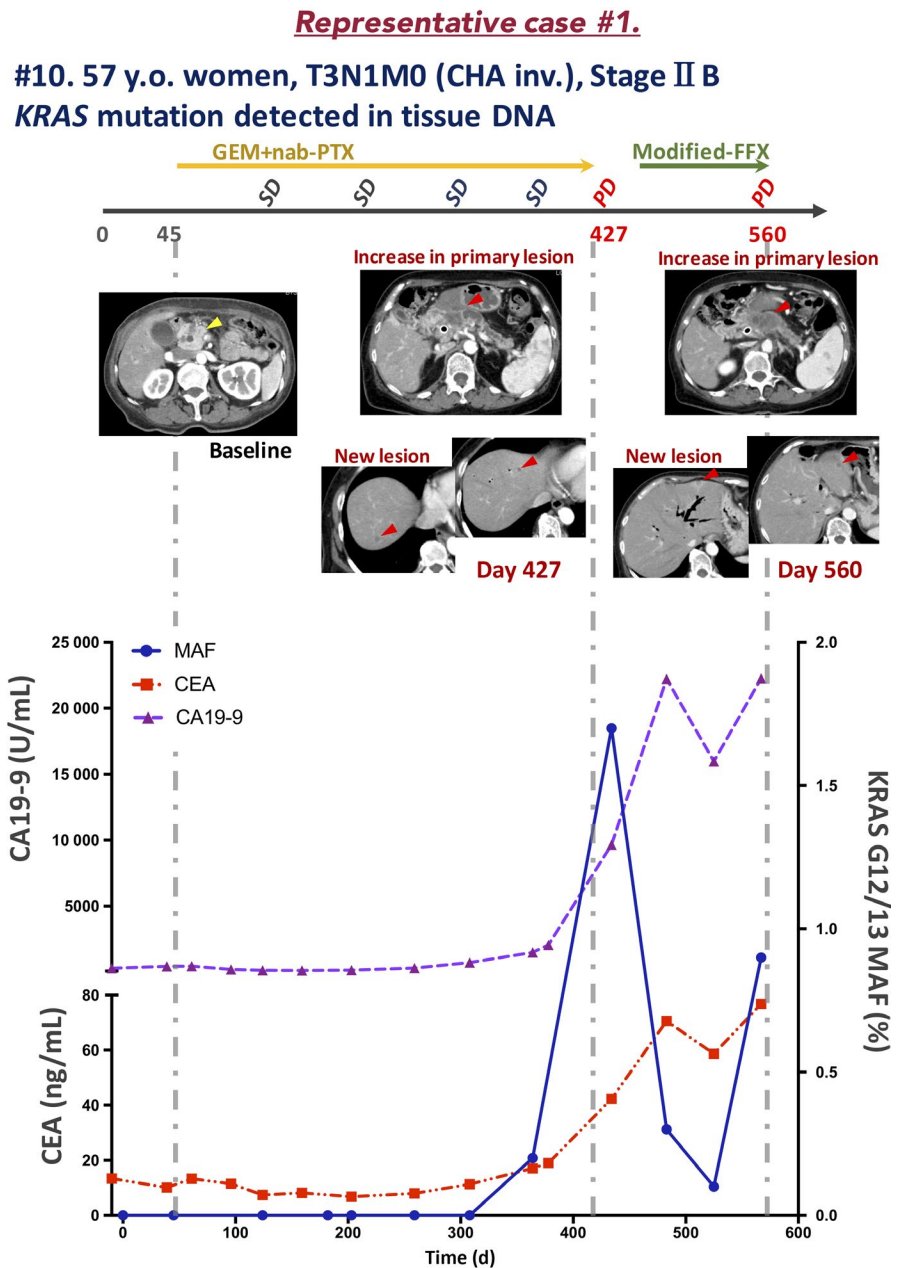
FIGURE 6 A, Changes in the *KRAS* mutation allele frequency (MAF) value and the carcinoembryonic antigen (CEA) and carbohydrate antigen 19-9 (CA19-9) levels before and after initial course of chemotherapy in pancreatic ductal adenocarcinoma cases in which the *KRAS* mutation disappeared (N = 8, Pat. #16, 17, 35, 36, 37, 38, 39, 40); cases in which the CEA or CA19-9 level was not elevated (CEA < 5.0 ng/mL, CA19-9 < 37.0 U/mL) were omitted. The *KRAS*-MAF value and the levels of CEA and CA19-9 were significantly decreased after initial course of chemotherapy. B, Changes in the *KRAS*-MAF value and the CEA and CA19-9 levels, 1 course of chemotherapy before and after first progressive disease (PD) in cases with *KRAS* mutation (N = 20); cases in which the CEA or CA19-9 level was not elevated (CEA < 5.0 ng/mL, CA19-9 < 37.0 U/mL) and no circulating tumor DNA sample obtained (Pat. #14) were omitted. At the time of the first PD, the *KRAS*-MAF value and the levels of CEA and CA19-9 were significantly increased. C, Changes of *KRAS*-MAF value (Δ *KRAS*-MAF) and those of the CEA and CA19-9 levels (%change) in each case. Δ *KRAS*-MAF significantly correlated with percentage change of CEA or CA19-9 levels

4 | DISCUSSION

In the current study, patients with distant metastasis except peritoneal metastasis showed a significantly higher *KRAS* mutation detection rate in ct-DNA compared to those with locally advanced disease or peritoneal metastasis. Also, in the patients without *KRAS* mutation in ct-DNA at the time of diagnosis, *KRAS* mutation was detected at the time of PD due to liver metastasis. In the Kaplan-Meier plot of PFS undergoing first-line chemotherapy, the patients with *KRAS* mutation in ct-DNA tended to have a worse PFS than those without (median, 308.5 vs 168 days, $P = .07$) (Figure 3C). Also, the patients with baseline tumor markers equal to or above the median value tended to have a worse PFS than those with baseline below the median value (CEA, median 244

vs 195 days, $P = .20$; CA19-9, median 281 vs 169 days, $P = .10$) (Figure 3A,3). Recently, the detection or the concentration of *KRAS* mutation in ct-DNA was reported to be one of the most reliable prognostic factors for survival in cases of advanced PDAC and for recurrence in cases of resected PDAC.²⁵⁻³⁰ Similarly, our data suggest that detection of *KRAS* mutation in ct-DNA or an elevated *KRAS*-MAF value indicates PD. Furthermore, up to 15%-26.4% of patients diagnosed with locally advanced PDAC by pre-operative CT had liver metastases by explorative laparoscopy.^{31,32} In our cohort, 2 locally advanced cases (without distant metastasis) showed *KRAS* mutation in ct-DNA and rapidly developed liver metastasis. Therefore, CT-occult metastases could exist at the time of diagnosis. These findings need to be verified in a prospective observational study.

FIGURE 7 Clinical course of a representative case of locally advanced pancreatic ductal adenocarcinoma (patient [Pat.] #10) in which circulating tumor DNA was monitored during chemotherapy. CA19-9, carbohydrate antigen 19-9; CEA, carcinoembryonic antigen; CHA inv., common hepatic artery invasion; FFX, FOLFIRINOX; GEM, gemcitabine; MAF, mutation allele frequency; nab-PTX, nab-paclitaxel; PD, progressive disease; SD, stable disease; y.o., years old



The utility of ct-DNA monitoring during chemotherapy is unclear due to the small number of cases analyzed.^{33,34} Two studies have assessed the relationship between changes in the levels of *KRAS* mutation in ct-DNA and disease progression. One showed that patients with *KRAS* mutation in ct-DNA after 1 month of chemotherapy treatment tended to have a worse PFS than those without.³⁵ The second reported a significant difference in PFS between patients displaying an increase vs decrease in the *KRAS* mutation level in ct-DNA at day 15 of first-line chemotherapy.³⁶ Interestingly, our results showed that, in cases with *KRAS* mutation in ct-DNA at the time of diagnosis, the *KRAS* mutation disappeared after the initial course of chemotherapy and reappeared concurrently with or earlier than PD (Pat. #16, 17, 35, 36, 37, 38, 39, 40) (Figure 4). In contrast, cases in which *KRAS* mutation remained after the initial course of chemotherapy (Pat. #32, 34, 37, 38, 41) showed a significantly worse PFS than those in whom it

disappeared (median 248.5 vs 50 days, $P = .001$) (Figure 5). Moreover, the changes in the *KRAS*-MAF value were concurrent with those in the CEA and CA19-9 levels (before vs after initial course of chemotherapy, and 1 course of chemotherapy before vs after first PD) and there was significant correlation between the change of *KRAS*-MAF values (Δ *KRAS*-MAF) and those of CEA and CA19-9 levels (%change) in each case with the above timings (Figure 6; Table S3). In cases in which the CEA or CA19-9 level was not elevated (CEA < 5.0 ng/mL, CA19-9 < 37.0 U/mL), which is often experienced in clinical practice (Tables 1 and 3; Table S1), the *KRAS*-MAF value might be more useful for monitoring *KRAS*-mutated PDAC during chemotherapy. Also, during monitoring of *NRAS* Q61R-mutated PDAC (a rare mutation in PDAC) (Figure S1) in patients without elevated CEA, CA19-9, Span-1, or Dupan-2 levels, the changes in the *NRAS*-MAF value seemed to be correlated with the disease state. Therefore, monitoring of

Representative case #2

**#39, 59 y.o. women, T4N1M1 (HEP, LYM, LUNG), Stage IV
KRAS mutation detected in tissue and ct-DNA**

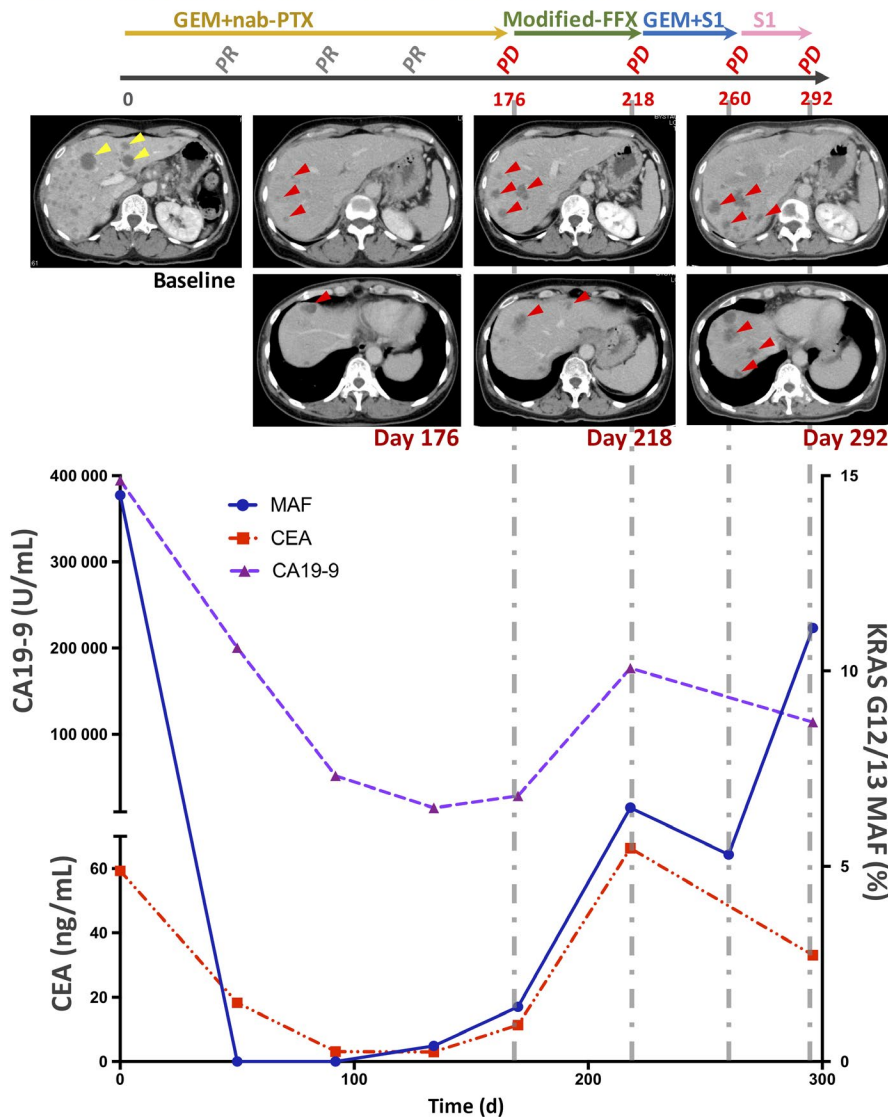


FIGURE 8 Clinical course of a representative case of pancreatic ductal adenocarcinoma with liver metastasis (patient [Pat.] #39). CA19-9, carbohydrate antigen 19-9; CEA, carcinoembryonic antigen; CHA inv., common hepatic artery invasion; FFX, FOLFIRINOX; GEM, gemcitabine; HEP, hepatic metastasis; LUNG, lung metastasis; LYM, lymphatic metastasis; MAF, mutation allele frequency; nab-PTX, nab-paclitaxel; PD, progressive disease; PR, partial response; S1, tegafur (a masked compound of 5-fluorouracil); y.o., years old

tumor-derived DNA enables continuous assessment of the disease state during chemotherapy.

Several prior studies have been aimed at detecting mutated *KRAS* in the ct-DNA of PDAC cases.²⁵ Using methods different from those in this study (ie, the dPCR probe, sample preparation [serum or plasma], and the sensitivity cut-off), *KRAS* mutation was detected at a high frequency in cases with distant metastasis, similar to our findings. In contrast, detection of mutated *KRAS* in patients with early PDAC is challenging. The previous fundamental study revealed circulating DNA is mainly excreted by the liver and kidney.³⁷ Therefore, tumor DNA derived from the primary pancreatic lesion is likely to be excreted in the liver and so is difficult to detect in peripheral blood. To define the lower limit of detection MAF value may enable to detect *KRAS* mutation in ct-DNA on the no-distant metastasis stage, however, it may worsen the specificity for the PDAC diagnosis, due to the existence of *KRAS* mutation detectable pancreatitis cases.^{38,39}

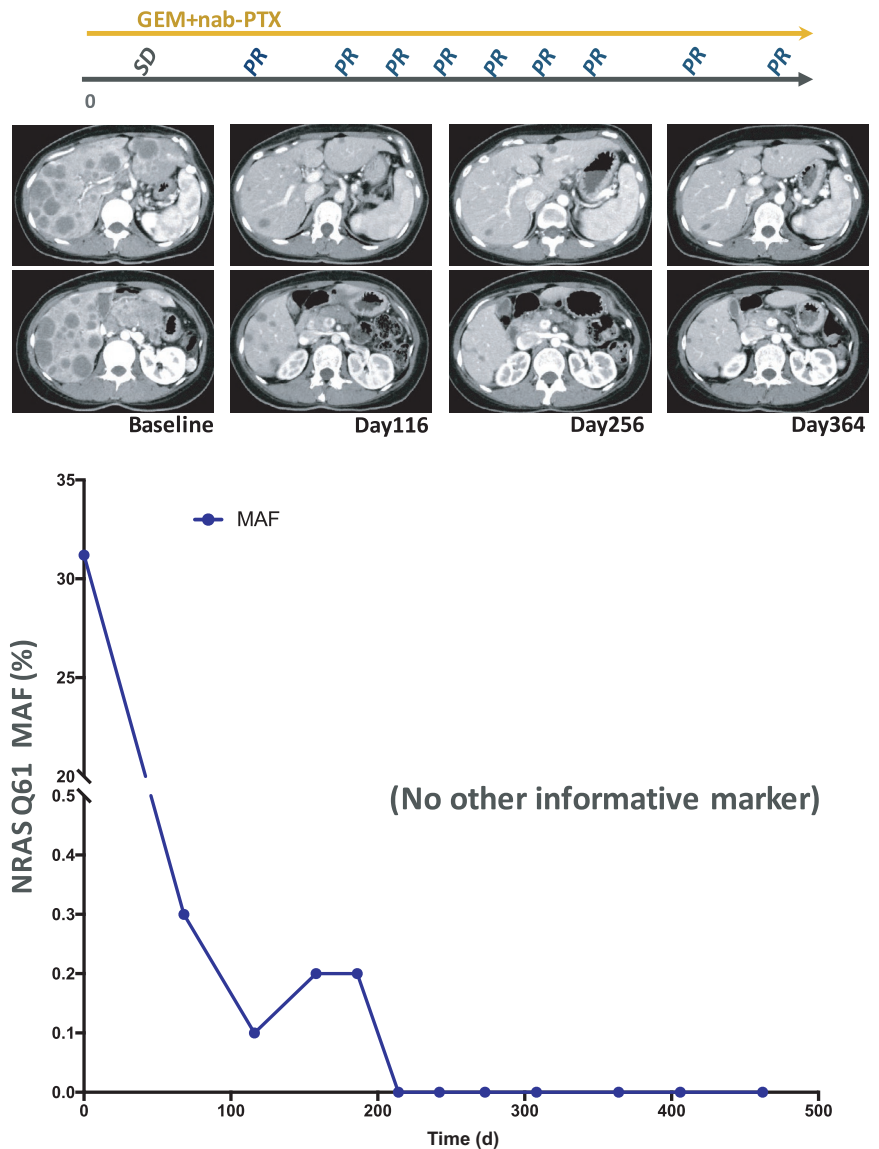
In a preliminary study, we detected mutated *KRAS* by dPCR in tissue samples of 2 of 17 cases of mass-forming pancreatitis.

Integration of the *KRAS*-MAF value and multiple markers reportedly improved the diagnostic accuracy of PDAC⁴⁰; however, there is no evidence supporting the clinical utility of ct-DNA detection for early-stage diagnosis.⁴¹ Compared to prior reports, *KRAS* mutation was detected in locally advanced or peritoneal metastatic PDAC cases at a low rate.^{25,27} This might be because we used a different probe (LBx probe for *KRAS* G12/13, which can detect 16 *KRAS* mutation patterns). However, the LBx probe for *KRAS* G12/13 enables the detection of more types of *KRAS* G12/13 mutations than other probes (Table S4). Another possibility is that we use ct-DNA extracted from serum, not plasma, samples. We believe that serum samples are easier to handle than other types of sample, including plasma.

In conclusion, the quantitative monitoring of ct-DNA by dPCR enables continuous evaluation of the disease state. Although further

FIGURE 9 Clinical course of a case of *NRAS*-mutated pancreatic ductal adenocarcinoma with liver metastasis (patient [Pat.] #47). ct-DNA, circulating tumor DNA; GEM, gemcitabine; HEP, hepatic metastasis; MAF, mutation allele frequency; nab-PTX, nab-paclitaxel; PER, peritoneal metastasis; PR, partial response; SD, stable disease; y.o., years old

Representative case #3
#47, 27 y.o. Women, T4N1M1 (HEP, PER) Stage IV
***NRAS* mutation detected in tissue and ct-DNA**



analysis is needed, the disappearance of *KRAS* mutation in ct-DNA during chemotherapy could be predictive factor for disease progression of patients with PDAC.

ACKNOWLEDGMENTS

Supported in part by a Grant-in-Aid for Scientific Research (KAKENHI).

DISCLOSURE STATEMENT

The authors declare that they have no conflicts of interest.

ORCID

Makoto Sugimori <https://orcid.org/0000-0001-5272-5167>

Takeshi Sato <https://orcid.org/0000-0002-5836-7273>

REFERENCES

- Rahib L, Smith BD, Aizenberg R, Rosenzweig AB, Fleshman JM, Matrisian LM. Projecting cancer incidence and deaths to 2030: the unexpected burden of thyroid, liver, and pancreas cancers in the United States. *Cancer Res.* 2014;74(11):2913-2921.
- Mitselos IV, Karoumpalis I, Theopistos VI, Tzilves D, Christodoulou DK. Endoscopic ultrasonography in pancreatic diseases: advances in tissue acquisition. *Endosc Int Open.* 2019;7(7):E922-E930.
- Fuccio L, Hassan C, Laterza L, et al. The role of K-ras gene mutation analysis in EUS-guided FNA cytology specimens for the differential diagnosis of pancreatic solid masses: a meta-analysis of prospective studies. *Gastrointest Endosc.* 2013;78(4):596-608.
- Hewitt MJ, McPhail MJ, Possamai L, Dhar A, Vlavianos P, Monahan KJ. EUS-guided FNA for diagnosis of solid pancreatic neoplasms: a meta-analysis. *Gastrointest Endosc.* 2012;75(2):319-331.
- Bailey P, Chang DK, Nones K, et al. Genomic analyses identify molecular subtypes of pancreatic cancer. *Nature.* 2016;531(7592):47-52.

6. Alexandrov LB, Nik-Zainal S, Wedge DC, et al. Signatures of mutational processes in human cancer. *Nature*. 2013;500(7463):415-421.
7. Biankin AV, Waddell N, Kassahn KS, et al. Pancreatic cancer genomes reveal aberrations in axon guidance pathway genes. *Nature*. 2012;491(7424):399-405.
8. Witkiewicz AK, McMillan EA, Balaji U, et al. Whole-exome sequencing of pancreatic cancer defines genetic diversity and therapeutic targets. *Nat Commun*. 2015;6:6744.
9. Eser S, Schnieke A, Schneider G, Saur D. Oncogenic KRAS signalling in pancreatic cancer. *Br J Cancer*. 2014;111(5):817-822.
10. Morris JP, Wang SC, Hebrok M. Wnt and the twisted developmental biology of pancreatic ductal adenocarcinoma. *Nat Rev Cancer*. 2010;10(10):683-695.
11. Kanda M, Matthaei H, Wu J, et al. Presence of somatic mutations in most early-stage pancreatic intraepithelial neoplasia. *Gastroenterology*. 2012;142(4):730-3.e9.
12. Trisolini E, Armellini E, Paganotti A, et al. KRAS mutation testing on all non-malignant diagnosis of pancreatic endoscopic ultrasound-guided fine-needle aspiration biopsies improves diagnostic accuracy. *Pathology*. 2017;49(4):379-386.
13. Sho S, Court CM, Kim S, et al. Digital PCR Improves Mutation Analysis in Pancreas Fine Needle Aspiration Biopsy Specimens. *PLoS ONE*. 2017;12(1):e0170897.
14. Bournet B, Selves J, Grand D, et al. Endoscopic ultrasound-guided fine-needle aspiration biopsy coupled with a KRAS mutation assay using allelic discrimination improves the diagnosis of pancreatic cancer. *J Clin Gastroenterol*. 2015;49(1):50-56.
15. de Biase D, Visani M, Baccarini P, et al. Next generation sequencing improves the accuracy of KRAS mutation analysis in endoscopic ultrasound fine needle aspiration pancreatic lesions. *PLoS ONE*. 2014;9(2):e87651.
16. Gleeson FC, Kerr SE, Kipp BR, et al. Targeted next generation sequencing of endoscopic ultrasound acquired cytology from ampullary and pancreatic adenocarcinoma has the potential to aid patient stratification for optimal therapy selection. *Oncotarget*. 2016;7(34):54526-54536.
17. Kameta E, Sugimori K, Kaneko T, et al. Diagnosis of pancreatic lesions collected by endoscopic ultrasound-guided fine-needle aspiration using next-generation sequencing. *Oncol Lett*. 2016;12(5):3875-3881.
18. Imaoka H, Sasaki M, Hashimoto Y, Watanabe K, Ikeda M. New era of endoscopic ultrasound-guided tissue acquisition: next-generation sequencing by endoscopic ultrasound-guided sampling for pancreatic cancer. *J Clin Med*. 2019;8(8):1173.
19. Leon SA, Shapiro B, Sklaroff DM, Yaros MJ. Free DNA in the serum of cancer patients and the effect of therapy. *Can Res*. 1977;37(3):646-650.
20. Diehl F, Schmidt K, Choti MA, et al. Circulating mutant DNA to assess tumor dynamics. *Nat Med*. 2008;14(9):985-990.
21. Ulrich BC, Paweletz CP. Cell-free DNA in oncology: gearing up for clinic. *Ann Lab Med*. 2018;38(1):1-8.
22. Barretina J, Caponigro G, Stransky N, et al. The cancer cell line encyclopedia enables predictive modelling of anticancer drug sensitivity. *Nature*. 2012;483(7391):603-607.
23. Gradiz R, Silva HC, Carvalho L, Botelho MF, Mota-Pinto A. MIA PaCa-2 and PANC-1 - pancreas ductal adenocarcinoma cell lines with neuroendocrine differentiation and somatostatin receptors. *Sci Rep*. 2016;6:21648.
24. Ozaka M, Ishii H, Sato T, et al. A phase II study of modified FOLFIRINOX for chemotherapy-naïve patients with metastatic pancreatic cancer. *Cancer Chemother Pharmacol*. 2018;81(6):1017-1023.
25. Kim MK, Woo SM, Park B, et al. Prognostic Implications of multiplex detection of KRAS mutations in cell-free DNA from patients with pancreatic ductal adenocarcinoma. *Clin Chem*. 2018;64(4):726-734.
26. Pietrasz D, Pécuchet N, Garlan F, et al. Plasma circulating tumor DNA in pancreatic cancer patients is a prognostic marker. *Clin Cancer Res*. 2017;23(1):116-123.
27. Bernard V, Kim DU, San Lucas FA, et al. Circulating nucleic acids are associated with outcomes of patients with pancreatic. *Cancer Gastroenterology*. 2019;156(1):pp. 108-18 e4.
28. Lee B, Lipton L, Cohen J, et al. Circulating tumor DNA as a potential marker of adjuvant chemotherapy benefit following surgery for localised pancreatic cancer. *Ann Oncol*. 2019.
29. Groot VP, Mosier S, Javed AA, et al. Circulating tumor DNA as a clinical test in resected pancreatic cancer. *Clin Cancer Res*. 2019.
30. Kinugasa H, Nouse K, Miyahara K, et al. Detection of K-ras gene mutation by liquid biopsy in patients with pancreatic cancer. *Cancer*. 2015;121(13):2271-2280.
31. Karabacak I, Satoi S, Yanagimoto H, et al. Risk factors for latent distant organ metastasis detected by staging laparoscopy in patients with radiologically defined locally advanced pancreatic ductal adenocarcinoma. *J Hepatobiliary Pancreat Sci*. 2016;23(12):750-755.
32. Liu X, Fu Y, Chen Q, et al. Predictors of distant metastasis on exploration in patients with potentially resectable pancreatic cancer. *BMC Gastroenterol*. 2018;18(1):168.
33. Perets R, Greenberg O, Shentzer T, et al. Mutant KRAS circulating tumor DNA is an accurate tool for pancreatic cancer monitoring. *Oncologist*. 2018;23(5):566-572.
34. Cheng HE, Liu C, Jiang J, et al. Analysis of ctDNA to predict prognosis and monitor treatment responses in metastatic pancreatic cancer patients. *Int J Cancer*. 2017;140(10):2344-2350.
35. Tjensvoll K, Lapin M, Buhl T, et al. Clinical relevance of circulating KRAS mutated DNA in plasma from patients with advanced pancreatic cancer. *Mol Oncol*. 2016;10(4):635-643.
36. Del Re M, Vivaldi C, Rofi E, et al. Early changes in plasma DNA levels of mutant KRAS as a sensitive marker of response to chemotherapy in pancreatic cancer. *Sci Rep*. 2017;7(1):7931.
37. Tsumita T, Iwanaga M. Fate of injected deoxyribonucleic acid in mice. *Nature*. 1963;198:1088-1089.
38. Lohr M, Kloppel G, Maisonneuve P, Lowenfels AB, Luttges J. Frequency of K-ras mutations in pancreatic intraductal neoplasias associated with pancreatic ductal adenocarcinoma and chronic pancreatitis: a meta-analysis. *Neoplasia*. 2005;7(1):17-23.
39. Le Calvez-Kelm F, Foll M, Wozniak MB, et al. KRAS mutations in blood circulating cell-free DNA: a pancreatic cancer case-control. *Oncotarget*. 2016;7(48):78827-78840.
40. Cohen JD, Javed AA, Thoburn C, et al. Combined circulating tumor DNA and protein biomarker-based liquid biopsy for the earlier detection of pancreatic cancers. *Proc Natl Acad Sci U S A*. 2017;114(38):10202-10207.
41. Sato Y, Matoba R, Kato K. Recent advances in liquid biopsy in precision oncology research. *Biol Pharm Bull*. 2019;42(3):337-342.

SUPPORTING INFORMATION

Additional supporting information may be found online in the Supporting Information section.

How to cite this article: Sugimori M, Sugimori K, Tsuchiya H, et al. Quantitative monitoring of circulating tumor DNA in patients with advanced pancreatic cancer undergoing chemotherapy. *Cancer Sci*. 2020;111:266–278. <https://doi.org/10.1111/cas.14245>